Asymmetric Flux Pinning in a Regular Array of Magnetic Dipoles

David J. Morgan[1] and J. B. Ketterson[1,2]
[1]*Department of Physics and Astronomy, Northwestern University, Evanston, Illinois 60208*
[2]*Department of Electrical and Computer Science, Northwestern University, Evanston, Illinois 60208*
(Received 5 September 1997)

The effect of a regular array of magnetic dipoles embedded in a superconducting film was investigated. A large asymmetry in critical currents was found between when the magnetic dipoles are aligned and antialigned with respect to an externally applied magnetic field. Enhanced pinning effects were observed when the flux lattice and the dipole lattice were commensurate. The data are used to infer pinning mechanisms, strengths, and sites. [S0031-9007(98)05817-7]

PACS numbers: 74.60.Jg, 74.60.Ge

Because of its intrinsic interest and technological relevance, flux pinning has been the subject of a vast amount of theoretical and experimental work. The introduction of artificial pinning sites has recently attracted interest. As an example, heavy ion-beam irradiation [1] has been used to create random columns of weakened superconductivity in YBCO. The associated regions of reduced condensation energy act as vortex pinning centers due to the energy savings from locating a vortex core on the columnar defect. A more controlled way to study pinning is to artificially pattern the pinning sites where the positions, size, and nature of the pinning sites may be "tuned" to some extent. Such ordered systems include regular arrays of holes [2] and in-plane magnetic particles [3,4], which have been defined with the aid of high resolution e-beam lithography. These ordered structures have shown peak effects in measurements of magnetization, critical current, and resistivity when the vortex density is a rational multiple of the artificial defect density which is referred to as commensurability. Experimentally, the pinning centers discussed in Refs. [3] and [4] behave symmetrically with respect to positive and negative applied perpendicular magnetic fields irrespective of their previous magnetic history.

The present paper describes measurements of the superconducting critical current of niobium films with an embedded array of ferromagnetic nickel particles. A key feature of this paper is that the aspect ratio (height/diameter) of the ferromagnetic particles is larger than in previous studies. Experimentally, we observe that the response of the film is strongly asymmetric with respect to the relative orientation between the applied perpendicular magnetic field and the embedded moments. This shows clearly that there is a vector contribution to the vortex pinning interaction. The strong asymmetry is particularly apparent in the commensurability effects between the defect lattice and the applied magnetic field. As opposed to previous studies, we also studied several lattice symmetries, where we observed significant differences in the commensurate peak structure. These data are exploited to suggest pinning mechanisms, strengths, and sites.

The system measured consists of a regular (square, triangular, and Kagomé) array of magnetic nickel dots (120 nm diameter by 110 nm height) covered by a film of niobium (95 nm thick by 80 μm wide). The regular arrays were defined by e-beam lithography in polymethylmethacrylate (PMMA) with a density δ of $(0.6\ \mu\mathrm{m})^{-2}$ and $(1.2\ \mu\mathrm{m})^{-2}$ over an area of $90\ \mu\mathrm{m} \times 90\ \mu\mathrm{m}$. Nickel was then deposited by e-beam evaporation followed by lift-off in acetone. The transport pattern was defined by: optical lithography, niobium deposition (by magnetron sputtering with a base pressure of 10^{-7} to 10^{-8}), and lift-off in acetone. The voltage leads are separated by 80 μm. No effort was made to remove any oxide barrier on the nickel dots prior to niobium deposition. The nickel dots thus perforate the film and have a niobium sheet on top. The superconducting transition temperatures were 8.60 ± 0.1 K (transition width of 0.015 K) for all samples, with and without Ni arrays, which implies no macroscopic reduction of T_c due to a magnetic or other proximity effects. From H_{c2} measurements, the mean free path, in the dirty limit, is $l \cong 45$ Å.

Transport measurements were performed in a Quantum Design ^{4}He cryostat equipped with a 5.5 T superconducting magnet. Current-voltage measurements were taken in a four-wire configuration, and critical currents were defined by a voltage criteria of 0.4 μV. In addition, at each new field setting, the current was ramped into the resistive (normal) region of the I-V characteristic to allow the flux lattice to redistribute more quickly to its new equilibrium position. To magnetize the nickel dots, a field of +3.5 T was applied perpendicular to the film plane. The field was then rapidly turned off. This magnetization procedure was performed prior to every field sweep since sweeping the field into negative fields (for positively magnetized samples) washed out some of the magnetic alignment. In what follows, a positive applied field is parallel to the initial magnetizing field, whereas a negative field is in the opposite direction.

Critical current I_c measurements as a function of magnetic field are shown in Figs. 1 and 2 for triangular magnetic dot arrays (with the above densities) at several temperatures. Both figures show a strong asymmetry for positive and negative applied fields. Strong commensurate peaks are also visible at the matching fields, $H_n = n\Phi_0\delta$,

 0031-9007/98/80(16)/3614(4)$15.00

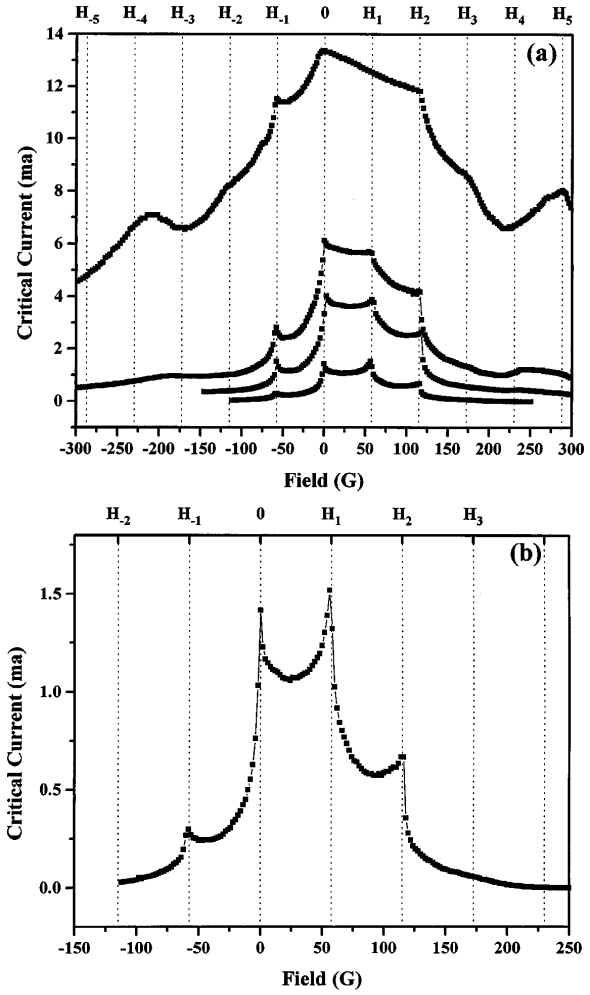

FIG. 1. (a) Critical current as a function of field for the high density triangular array at $T = 8.00$, 8.40, 8.46, and 8.52 K (top to bottom) ($T_c = 8.56$ K). (b) Enlargement of the $T = 8.52$ K sweep.

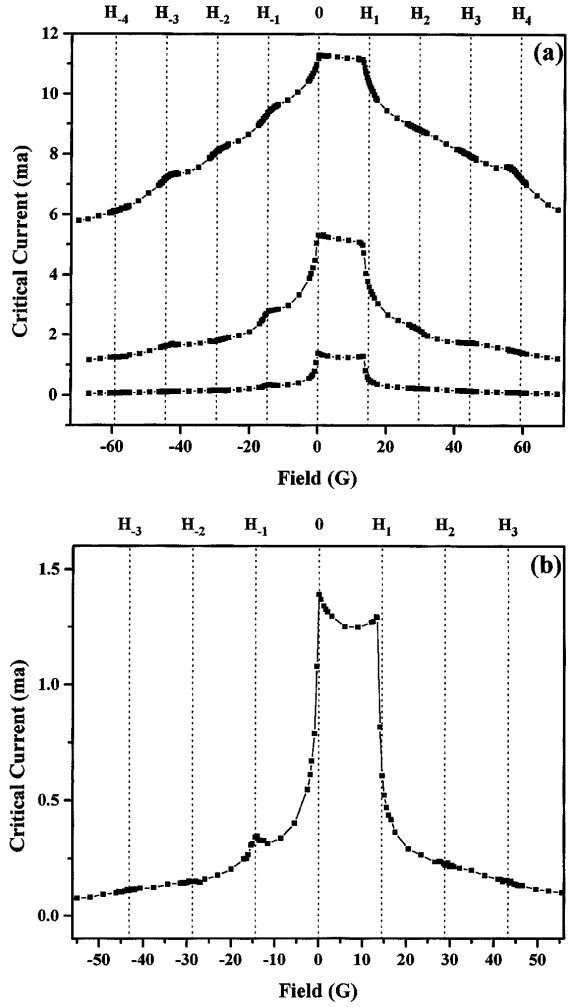

FIG. 2. (a) Critical current as a function of field for the low density triangular array at $T = 8.00$, 8.50, and 8.64 K (top to bottom) ($T_c = 8.69$ K). (b) Enlargement of the $T = 8.64$ K sweep.

where n is the number of vortices per magnetic defect. The vertical lines indicate integer multiples of the first commensurate field (14.4 and 57.5 G for the low and high density array, respectively). We also verified that magnetizing the sample in the opposite direction gave mirror results to those shown. Measurements of unmagnetized samples (not shown) showed a field-symmetric behavior which was not, however, the simple average of the positive and negative field behavior of the magnetized sample. The unmagnetized behavior is more complicated due to the presence of magnetic disorder.

An interesting feature of the data in Figs. 1 and 2 is the cusplike structure of I_c observed for the high density dot array near T_c: The low density array is far more flat (field independent) up to the first commensurate field H_{+1} at all temperatures (except very near T_c, where some cusp structure is present). In fact, all I_c field sweeps for the low density array have exactly the same slope up to H_{+1}: $dI_c/dB = -0.02$ ma/G. This nearly field-independent structure for the low density array can be understood if the pinning is very strong (up to H_{+1}) and the pinning density is low enough that a pinned vortex does not interact with a neighboring defect or another pinned vortex. Simulations demonstrate [5] that, if this pinning strength is above a threshold f_p, the vortices should be immobilized for all transport current densities. The onset of resistivity would then be associated with some mechanism other than flux flow (e.g., depairing), resulting in very little field dependence of the critical current density. In this case, we should not see a flux flow regime, but rather a sharp transition to the resistive state. Experimentally, we find that, indeed, within the resolution of the data taken, the resistive transition is steplike for fields up to H_{+1} (except very near T_c). Immediately above H_{+1} the transition broadens increasingly with field. Note that the falloff in the critical current with field shown can be accounted for if one considers the reduction in the cross-sectional are due to the inclusion of the vortices normal cores of width ξ. The temperature independence of the slope is explained by considering that empirically we find that the zero field

critical current scales as $(1 - T/T_c)^{1/2}$ while the width of the normal cores scale with the temperature-dependent coherence length, $(1 - T/T_c)^{1/2}$. This effectively cancels any temperature dependence of the slope. Calculations based upon these considerations show excellent agreement with the measured data.

Alternately, the cusp structure of the high density array may be interpreted as a pinning force less than f_p. This reduced pinning strength behavior is much more pronounced as the temperature approaches T_c. Two factors could contribute to this behavior. First, vortex-vortex interactions become more important due to the increasing London depth with temperature and the increased proximity of neighboring pinning sites. If two neighboring pinning sites are each occupied by a single vortex, while another neighboring site is not, the pinning strength is reduced from the vortex-vortex repulsion and the vortex–vacant-site attraction. This instability should increase with the defect density and the London depth. Second, the spatial range of a magnetic dot's potential well should increase with the London depth and coherence length, thereby potentially overlapping nearby wells. Again, this reduces the strength of a given pinning center by reducing the effective depth of the well potential. The net effect is that the pinning strength is reduced for higher density magnetic dot arrays near T_c. Only at the first commensurate field H_{+1}, where every pinning defect is occupied by one vortex, do we expect and see a strong increase in the critical current. This configuration, stabilized by the mutual repulsion of the vortices and the absence of any vacant pinning sites, has been argued to be analogous to a Mott insulator phase [6]. If the overlap argument above is correct, one would expect the cusp structure to diminish with decreasing T, eventually approaching the behavior of the low density array. This is exactly what is seen in Fig. 1(a), where, with decreasing T, the cusp structure flattens and eventually exhibits the same constant slope (of about -0.02 ma/G) as the low density array (some samples had slightly different slopes, but when the slope was normalized by the observed critical current the same value was obtained). The resistive transition, at 8.0 K, is abrupt for fields up to H_{+2} within the resolution of the data taken. This is seen in Fig. 3, where each line (at a given temperature) represents a different voltage criteria for the critical current.

The observed asymmetric pinning is consistent with that expected from the interaction energy between a dipole and an external magnetic field, $E = -\vec{\mu} \cdot \vec{H}$. Since the field of a vortex increases with decreasing r, the vortex can lower its energy by moving closer to a magnetic moment which is aligned parallel to the vortex field. Therefore the force is attractive for the aligned case. The opposite is true for the case of an antialigned field and moment. Early theoretical studies [7] on the interaction of a magnetic moment and a vortex displaced a distance R used a Gibbs free energy argument to show, semiquantitatively, that the force was attractive. More recent studies [8] examined the fringing field from a vortex and its interaction with a magnetic moment above the superconductor in connection with magnetic force microscopy. However, it was assumed that the magnetic moment does not induce currents in the superconductor or disturb the magnetic field produced by a vortex which is not valid when the magnetic particle is close to the superconductor. Numerical solutions [9] of the Ginzburg-Landau equations have been obtained for the field and current distribution around a magnetic moment embedded in and aligned perpendicular to the plane of a superconductor. The pinning force between a vortex and an embedded magnetic dipole consists of at least three contributions: (i) the interaction between the vortex fringing field and magnetic moment, (ii) the interaction between a vortex and the screening currents created in response to the magnetic dipole, and (iii) the interaction of a vortex core with an area of reduced condensation energy, where this area is comprised of a void at the defect and a surrounding annulus due to the proximity effect (if the moment and the film are in electrical contact) and the screening current response to the dipole fringing field [3,9]. All of these interactions are, to varying degrees, mutually dependent, requiring a self-consistent treatment. The first two are vector interactions, which depend on the relative orientation of the vortex and the dipole. These should cause the asymmetry seen in our work. The third category involves scalar interactions and thus should not depend on the relative orientation, and would be attractive. For an antialigned moment and applied field, the last category competes with the first two and could result in interstitial sites dominating over defect pinning. In the following we will infer the strength of the magnetic pinning sites by looking at different defect lattices.

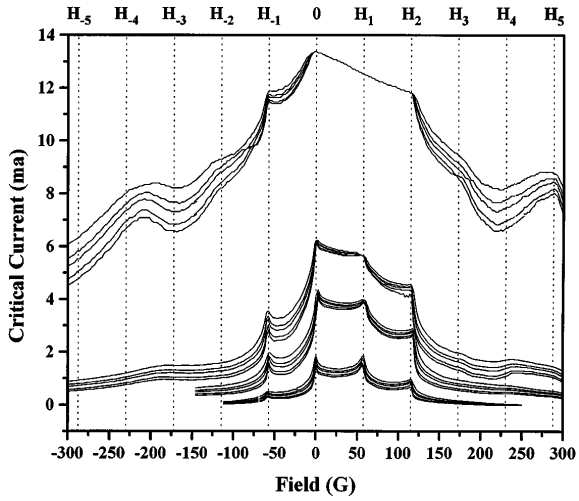

FIG. 3. Lines of constant voltage for the high density array at 8.00, 8.40, 8.46, and 8.52 K (top to bottom). The lines at a given temperature correspond to 0.4, 1, 3, 5, and 10 μV (top to bottom) voltage criteria for the critical current.

Stability analysis indicates and simulations [10] verify that, depending on the strength of the pinning and the defect lattice symmetry, certain commensurate peaks may be absent. For weaker pinning, a triangular lattice should

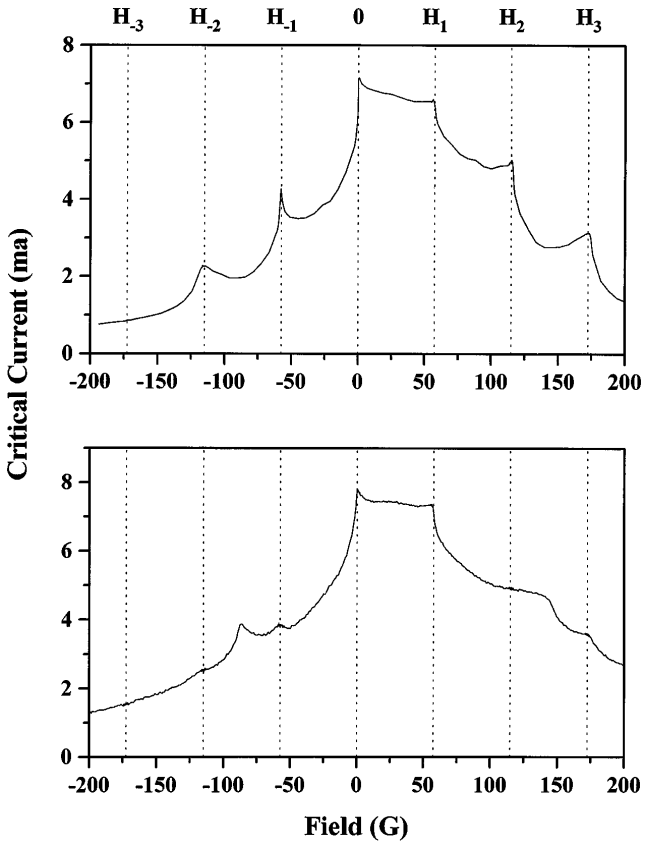

FIG. 4. Critical current as a function of field for the square (top) and Kagomé (bottom) arrays.

show peaks at H_1, H_3 while a square lattice should show peaks at $H_1, H_2, H_4 \ldots$. The simulations also show that the H_1 peak should be absent in a Kagomé lattice. We can exploit these missing peaks in Figs. 1 and 4 (critical current sweeps for a square and a Kagomé array) to infer the strength of the magnetic moment pinning sites for the higher density array (the lower density arrays do not show strong peaks past H_{+1}, possibly due to diminished collective effects or reduced interstitial pinning). Starting with the antialigned situation, we see the H_{-1} peak in all cases. This peak is not expected in the Kagomé and triangular lattices if the vortices were pinned in the interstitial sites. Stable interstitial pinning should show peaks at $H_{-1/2}$ and H_{-2}, respectively. We therefore conjecture that the vortices are pinned on the magnetic dots at H_{-1} and infer that the scalar interactions [case (iii)] discussed above are stronger than the two vector interactions [cases (i) and (ii)]. For the aligned case, we see that the H_{+3} peak is absent rather than the predicted H_{+2} peak for the triangular array. This would imply a doubly quantized pin at H_{+2}. The H_{+4} peak would then come from the doubly pinned dot with the next two vortices at the two equivalent interstitial sites. This doubly quantized interpretation is consistent with the data from the square lattice, where we see the H_{+3} peak which, again, is not predicted. This peak is most likely from the single interstitial pinning site after the dots become doubly quantized. Interestingly, a strong H_{+2} peak is not seen for the Kagomé lattice but rather one at $H_{+2\,1/2}$. This can only come from doubly quantized defects plus one vortex per interstitial (the interstitial density in the Kagomé lattice is half that of the defect lattice). These multiply quantized magnetic pinning sites are analogous to the multiply quantized holes discussed in Refs. [11] and [12], where the number of vortices a hole can pin is related to the hole radius. A similar analysis for the number of vortices a magnetic dot can pin should also be possible.

In conclusion, we have demonstrated that magnetic dipoles are very strong pinning centers in superconductors and that the strength depends on the relative alignment between the dipoles and the vortices. This results in a strong asymmetry between critical currents for aligned and antialigned magnetic fields. What is needed now is a theoretical analysis of the self-consistent magnetic and superconducting response of this system.

We would like to thank S. Patashinski, P. R. Auvil, S. K. Yip, and J. Clem for helpful suggestions. This work was supported by the Northwestern Materials Research Center under NSF Grant No. DMR9309061 and the Army Research Organization under Grant No. DAAG55-97-1-0133.

[1] L. Civale, A. D. Marwick, T. K. Worthington, M. A. Kirk, J. R. Thompson, L. Krusin-Elbaum, Y. Sun, J. R. Clem, and F. Holtzberg, Phys. Rev. Lett. **67**, 648 (1991).
[2] M. Baert, V. V. Metlushko, R. Jonckheere, V. V. Moshchalkov, and Y. Bruynseraede, Phys. Rev. Lett. **74**, 3269 (1995).
[3] Y. Nozaki, Y. Otani, K. Runge, H. Miyajima, B. Pannetier, J. P. Nozières, and G. Fillion, J. Phys. **79**, 8571 (1996).
[4] J. I. Martin, M. Vélez, J. Nogués, and Ivan K. Schuller, Phys. Rev. Lett. **79**, 1929 (1997).
[5] C. Reichhardt, C. J. Olson, J. Groth, S. Field, and F. Nori, Phys. Rev. B **53**, R8898 (1996).
[6] D. R. Nelson and V. M. Vinokur, Phys. Rev. B **48**, 13 060 (1993).
[7] S. H. Autler, J. Low Temp. Phys. **9**, 241 (1972).
[8] M. W. Coffey and E. T. Phipps, Phys. Rev. B **53**, 389 (1996).
[9] I. K. Marmorkos, A. Matulis, and F. M. Peeters, Phys. Rev. B **53**, 2677 (1996).
[10] C. Reichhardt, J. Groth, C. J. Olson, S. Field, and F. Nori, Phys. Rev. B **54**, 16 108 (1996).
[11] A. I. Buzdin, Phys. Rev. B **47**, 11 416 (1993).
[12] G. S. Mkrtchyan and V. V. Shmidt, JETP **34**, 195 (1972).